REPORT DOCUMENTATION PAGE

Form Approved OMB NO. 0704-0188

The public reporting burden for this collection of information is estimated to average 1 hour per response, including the time for reviewing instructions, searching existing data sources, gathering and maintaining the data needed, and completing and reviewing the collection of information. Send comments regarding this burden estimate or any other aspect of this collection of information, including suggesstions for reducing this burden, to Washington Headquarters Services, Directorate for Information Operations and Reports, 1215 Jefferson Davis Highway, Suite 1204, Arlington VA, 22202-4302. Respondents should be aware that notwithstanding any other provision of law, no person shall be subject to any oenalty for failing to comply with a collection of information if it does not display a currently valid OMB control number.
PLEASE DO NOT RETURN YOUR FORM TO THE ABOVE ADDRESS.

1. REPORT DATE (DD-MM-YYYY)	2. REPORT TYPE	3. DATES COVERED (From - To)
07-09-2015	Final Report	1-Sep-2010 - 31-Aug-2014

4. TITLE AND SUBTITLE
Final Report: Integrated Analysis of Piezoelectric Resonators as Components of Electronic Systems

5a. CONTRACT NUMBER
W911NF-10-1-0293

5b. GRANT NUMBER

5c. PROGRAM ELEMENT NUMBER
611102

6. AUTHORS
Haifeng Zhang, Jiashi Yang

5d. PROJECT NUMBER

5e. TASK NUMBER

5f. WORK UNIT NUMBER

7. PERFORMING ORGANIZATION NAMES AND ADDRESSES
University of North Texas
1155 Union Circle #305250

Denton, TX -

8. PERFORMING ORGANIZATION REPORT NUMBER

9. SPONSORING/MONITORING AGENCY NAME(S) AND ADDRESS (ES)
U.S. Army Research Office
P.O. Box 12211
Research Triangle Park, NC 27709-2211

10. SPONSOR/MONITOR'S ACRONYM(S)
ARO

11. SPONSOR/MONITOR'S REPORT NUMBER(S)
57792-EL.37

12. DISTRIBUTION AVAILIBILITY STATEMENT
Approved for Public Release; Distribution Unlimited

13. SUPPLEMENTARY NOTES
The views, opinions and/or findings contained in this report are those of the author(s) and should not contrued as an official Department of the Army position, policy or decision, unless so designated by other documentation.

14. ABSTRACT
The goal of this project was to develop a quantitative analysis software tool that links materials and advanced design to communication, navigation, and surveillance system performance. The project began on Sept. 1, 2010 and ended on Aug 31, 2014, and included a one-year no-cost extension. We have completed the software package and, in the process, we have performed both experimental measurement and theoretical analysis for quartz/langasite resonators. Our work resulted in 23 journal papers and 3 conference publications. The software package helped shorten the design cycle of a military electronic system. Our experiment and theoretical modeling results so far

15. SUBJECT TERMS
Resonators, third order elastic constants, quartz

16. SECURITY CLASSIFICATION OF:			17. LIMITATION OF ABSTRACT	15. NUMBER OF PAGES	19a. NAME OF RESPONSIBLE PERSON
a. REPORT	b. ABSTRACT	c. THIS PAGE			Haifeng Zhang
UU	UU	UU	UU		19b. TELEPHONE NUMBER 940-369-8266

Standard Form 298 (Rev 8/98)
Prescribed by ANSI Std. Z39.18

Report Title

Final Report: Integrated Analysis of Piezoelectric Resonators as Components of Electronic Systems

ABSTRACT

The goal of this project was to develop a quantitative analysis software tool that links materials and advanced design to communication, navigation, and surveillance system performance. The project began on Sept. 1, 2010 and ended on Aug 31, 2014, and included a one-year no-cost extension. We have completed the software package and, in the process, we have performed both experimental measurement and theoretical analysis for quartz/langasite resonators. Our work resulted in 23 journal papers and 3 conference publications. The software package helped shorten the design cycle of a military electronic system. Our experiment and theoretical modeling results so far provide new knowledge about resonator design and therefore have potentially reduced the design cycle of future military electronic systems.

Enter List of papers submitted or published that acknowledge ARO support from the start of the project to the date of this printing. List the papers, including journal references, in the following categories:

(a) Papers published in peer-reviewed journals (N/A for none)

Received		Paper
08/30/2011	2.00	Haifeng Zhang. Optimal cuts to extract the third-order elastic constants of langasite single crystals, IEEE Transactions on Ultrasonics, Ferroelectrics, and Frequency Control, (06 2011): 1245. doi:
08/30/2012	4.00	Huijing He, Jiashi Yang, John A. Kosinski. Shear-horizontal vibration modes of an oblate elliptical cylinder and energy trapping in contoured acoustic wave resonators, IEEE Transactions on Ultrasonics, Ferroelectrics, and Frequency Control, (08 2012): 1774. doi:
08/30/2012	9.00	Guijia Chen, Rongxing Wu, Ji Wang, Jianke Du,, Jiashi Yang. Five-Mode Frequency Spectra of x3-DependentModes in AT-Cut Quartz Resonators, IEEE TRANSACTIONS ON Ultrasonics, Ferroelectrics, and Frequency Control, 52, 1461-1467 (2005)., (04 2012): 811. doi:
09/10/2012	10.00	N Liu, J S Yang, F Jin. Transient thickness-shear vibration of a piezoelectric plate of monoclinic crystals, International Journal of Applied electromagetics and mechanics, (01 2012): 27. doi:
09/11/2013	15.00	Haifeng Zhang. Analysis of Thickness Vibrations of C-Axis Inclined Zig-Zag Multi-layered Zinc Oxide Thin Film Resonators, Ferroelectrics, (01 2013): 0. doi: 10.1080/00150193.2013.814251
09/11/2013	17.00	Haifeng Zhang. Optimal cuts to extract the third-order piezoelectric constants and electrostictive constants of langasite single crystals through the electroelastic effect, IEEE Transactions on Ultrasonics, Ferroelectrics and Frequency Control, (07 2013): 0. doi: 10.1109 /TUFFC.2013.2717
09/11/2013	18.00	Haifeng Zhang, Joseph Turner, John Kosinski. Experimental measurements of the force¿frequency effect of thickness-mode langasite resonators, IEEE Transactions on Ultrasonics, Ferroelectrics and Frequency Control, (07 2013): 0. doi: 10.1109 /TUFFC.2013.2719
09/11/2013	21.00	Peng Li, Feng Jin, Jiashi Yang. Thickness-shear vibration of an AT-cut quartz resonator with a hyperbolic contour, IEEE Transactions on Ultrasonics, Ferroelectrics and Frequency Control, (05 2012): 0. doi: 10.1109 /TUFFC.2012.2286
09/11/2013	22.00	Guijia Chen, Rongxing Wu, Ji Wang, Jianke Du, Jiashi Yang. Five-mode frequency spectra of x₃-dependent modes in AT-cut quartz resonators, IEEE Transactions on Ultrasonics, Ferroelectrics and Frequency Control, (04 2012): 0. doi: 10.1109 /TUFFC.2012.2259
09/11/2013	23.00	Nan Liu, Jiashi Yang, Ji Wang. Analysis of a monolithic, two-dimensional array of quartz crystal microbalances loaded by mass layers with nonuniform thickness, IEEE Transactions on Ultrasonics, Ferroelectrics and Frequency Control, (04 2012): 0. doi: 10.1109 /TUFFC.2012.2252
11/30/2014	25.00	Jun Zhu, Weiqiu Chen, Jiashi Yang. Overtone frequency spectra for ξ₃-dependent modes in AT-cut quartz resonators [Correspondence], IEEE Transactions on Ultrasonics, Ferroelectrics and Frequency Control, (04 2013): 0. doi: 10.1109 /TUFFC.2013.2636

11/30/2014 24.00 Huijing He, Jiashi Yang, John A. Kosinski, Ji Wang. Thickness-shear vibration of a rectangular quartz plate with partial electrodes,
Acta Mechanica Solida Sinica, (04 2013): 0. doi: 10.1016/S0894-9166(13)60012-9

11/30/2014 26.00 Huijing He, Jinxi Liu, Jiashi Yang. Thickness-shear and thickness-twist vibrations of an AT-Cut quartz mesa resonator,
IEEE Transactions on Ultrasonics, Ferroelectrics and Frequency Control, (10 2011): 0. doi: 10.1109 /TUFFC.2011.2055

11/30/2014 27.00 Junjie Shi, Cuiying Fan, Minghao Zhao, Jiashi Yang. Variational formulation of the Stevens-Tiersten equation and application in the analysis of rectangular trapped-energy quartz resonators,
The Journal of the Acoustical Society of America, (01 2014): 0. doi: 10.1121/1.4829535

11/30/2014 28.00 Wenjun Wang, Rongxing Wu, Ji Wang, Jianke Du, Jiashi Yang. Thickness-shear modes of an elliptical, contoured at-cut quartz resonator,
IEEE Transactions on Ultrasonics, Ferroelectrics, and Frequency Control, (06 2013): 0. doi: 10.1109 /TUFFC.2013.2681

11/30/2014 29.00 Hui-Jing He, Jia-Shi Yang, Wei-Ping Zhang, Ji Wang. Effects of mode coupling on the admittance of an AT-cut quartz thickness-shear resonator,
Chin. Phys. B, (04 2013): 0. doi: 10.1088/1674-1056/22/4/047702

11/30/2014 30.00 Nan Liua, Jiashi Yang, Feng Jin. Transient thickness-shear vibration of apiezoelectric plate of monoclinic crystals,
International Journal of Applied Electromagnetics and Mechanics 38 (2012) 27–37, (02 2012): 27. doi:

11/30/2014 31.00 Zhi Wang, Minghao Zhao, Jiashi Yang. Amplitude evolution equation and transient effects in piezoelectric crystal resonators,
Journal of Applied Physics, (10 2013): 0. doi: 10.1063/1.4825050

11/30/2014 34.00 Haifeng Zhang, Yuanye Bao. Sensitivity analysis of multi-layered C-axis inclined zigzag zinc oxide thin-film resonators as viscosity sensors,
IEEE Transactions on Ultrasonics, Ferroelectrics, and Frequency Control, (03 2014): 0. doi: 10.1109 /TUFFC.2014.2936

11/30/2014 35.00 Haifeng Zhang, Karim Afzalul. Design and analysis of a connected broadband multi-piezoelectric-bimorph- beam energy harvester,
IEEE Transactions on Ultrasonics, Ferroelectrics, and Frequency Control, (06 2014): 0. doi: 10.1109 /TUFFC.2014.2997

11/30/2014 36.00 Haifeng Zhang, Mehdi Ahmadi. Resonance Tuning of a Multi-piezoelectric Bimorph Beams Energy Harvester Connected by Springs,
Ferroelectrics, (02 2014): 0. doi: 10.1080/00150193.2014.874898

TOTAL: 21

Number of Papers published in peer-reviewed journals:

(b) Papers published in non-peer-reviewed journals (N/A for none)

Received	Paper
09/11/2013 12.00	Haifeng Zhang, John A. Kosinski, Yuan Xie, and Joseph A. Turner. Drive-Level Dependence of Doubly Rotated Langasite Resonators With Different Configurations, IEEE TRANSACTIONS ON Ultrasonics, Ferroelectrics, and Frequency Control, (05 2013): 963. doi:
09/11/2013 11.00	Haifeng Zhang and John A. Kosinski. Analysis of Thickness Vibrations ofC-Axis Inclined Zig-Zag Two-LayeredZinc Oxide Thin-Film Resonators, IEEE TRANSACTIONS ON Ultrasonics, Ferroelectrics, and Frequency Control, (12 2012): 2831. doi:
09/11/2013 13.00	Haifeng Zhang and John A. Kosinski. Analysis of Contributions of Nonlinear Material Constants to Stress-Induced elocity Shifts of Quartz and Langasite Surface Acoustic Wave Resonators, IEEE TRANSACTIONS ON Ultrasonics, Ferroelectrics, and Frequency Control, (05 2013): 60. doi:
09/11/2013 14.00	Haifeng Zhang, Joseph A. Turner, Jiashi Yang, John A. Kosinski, and Yuanye Bao. Experimental Measurement of the electroelastic Effect in Thickness-Mode Langasite Resonators , IEEE Transactions on Ultrasonics, Ferroelectrics, and Frequency Control, (05 2013): 60. doi:
09/11/2013 16.00	Haifeng Zhang, J. A. Kosinski, and Md. Afzalul Karim. Apparatus for measurement of acoustic wave propagation under uniaxial loading with application to measurement of third-order elastic constants of piezoelectric single crystals, Review of Scientific Instruments, (07 2013): 1. doi:
09/11/2013 19.00	Yumei Chena, Ji Wanga, Jianke Dua and Jiashi Yang. Shear-horizontal waves in a rotatedY-cut quartz plate on an elastic halfspace, Philosophical Magazine Letters, (02 2012): 77. doi:
09/16/2013 20.00	Nan Liu, Jiashi Yang, Feng Jin . Transient thickness-shear vibration of a piezoelectric plate of monoclinic crystals , International Journal of Applied Electromagnetics and Mechanics, (01 2012): 27. doi:
TOTAL:	**7**

Number of Papers published in non peer-reviewed journals:

(c) Presentations

Number of Presentations: 0.00

Non Peer-Reviewed Conference Proceeding publications (other than abstracts):

Received		Paper
08/30/2012	3.00	Haifeng Zhang, Montz B.D. , Tinghui Fan , Kosinski J.A. . Wireless Langasite Resonator as a Force Sensor, 2012 International frequency control symposium. 21-MAY-12, . : ,
TOTAL:	**1**	

Number of Non Peer-Reviewed Conference Proceeding publications (other than abstracts):

Peer-Reviewed Conference Proceeding publications (other than abstracts):

Received		Paper
08/30/2011	1.00	Haifeng Zhang, , Yuan Xie,, Joseph A. Turner,, John A. Kosinski.. Drive level dependence of doubly rotated langasite resonators with different configurations, 2011 International Frequency Control Symposium. 02-MAY-11, . : ,
11/30/2014	32.00	J. A. Kosinski, H. F. Zhang, Y. Y. Bao. MEASUREMENT OF THE SECOND ORDER ELASTIC CONSTANTS OF LANGASITE CRYSTALS, ASME 2014 Smart Materials, Adaptive Structures and Intelligent Systems . 08-SEP-14, . : ,
11/30/2014	33.00	Haifeng Zhang, Tinghui Fan. A wireless electric field sensor based on a langasite resonator, 2013 Joint European Frequency and Time Forum & International Frequency Control Symposium (EFTF/IFC). 20-JUL-13, Prague, Czech Republic. : ,
TOTAL:	**3**	

Number of Peer-Reviewed Conference Proceeding publications (other than abstracts):

(d) Manuscripts

Received		Paper
08/30/2012	5.00	H. F. Zhang, Pouhua Lee, John A. Kosinski. Experimental Study of A Frequency-Adjustable Piezoelectric Bimorph Energy Harvester, Integrated Ferroelectrics (06 2012)
08/30/2012	6.00	Haifeng Zhang, John A. Kosinski. Analysis of Thickness Vibrations of C-Axis Inclined Zig-zag Two-layered Zinc Oxide Thin Film Resonators, IEEE Transactions on Ultrasonics, Ferroelectrics, and Frequency Control (06 2012)
08/30/2012	7.00	Haifeng Zhang, John A. Kosinski, Yuan Xie , Joseph A. Turnerd. Drive Level Dependence of Doubly Rotated Langasite Resonators withDifferent Configurations, IEEE Transactions on Ultrasonics, Ferroelectrics, and Frequency Control (06 2012)
TOTAL:		**3**

Number of Manuscripts:

Books

Received	Book
TOTAL:	

Received	Book Chapter
TOTAL:	

Patents Submitted

Patents Awarded

Awards

Graduate Students

NAME	PERCENT_SUPPORTED	Discipline
Karim Afazul	1.00	
Mehdi Ahmadi	0.50	
Lijun Yang	0.50	
Huijin He	1.00	
FTE Equivalent:	**3.00**	
Total Number:	**4**	

Names of Post Doctorates

NAME	PERCENT_SUPPORTED
FTE Equivalent:	
Total Number:	

Names of Faculty Supported

NAME	PERCENT_SUPPORTED	National Academy Member
Haifeng Zhang	1.00	
Jiashi Yang	1.00	
FTE Equivalent:	**2.00**	
Total Number:	**2**	

Names of Under Graduate students supported

NAME	PERCENT_SUPPORTED
FTE Equivalent:	
Total Number:	

Student Metrics

This section only applies to graduating undergraduates supported by this agreement in this reporting period

The number of undergraduates funded by this agreement who graduated during this period:	4.00
The number of undergraduates funded by this agreement who graduated during this period with a degree in science, mathematics, engineering, or technology fields:	2.00
The number of undergraduates funded by your agreement who graduated during this period and will continue to pursue a graduate or Ph.D. degree in science, mathematics, engineering, or technology fields:	0.00
Number of graduating undergraduates who achieved a 3.5 GPA to 4.0 (4.0 max scale):	3.00
Number of graduating undergraduates funded by a DoD funded Center of Excellence grant for Education, Research and Engineering:	0.00
The number of undergraduates funded by your agreement who graduated during this period and intend to work for the Department of Defense	0.00
The number of undergraduates funded by your agreement who graduated during this period and will receive scholarships or fellowships for further studies in science, mathematics, engineering or technology fields:	0.00

Names of Personnel receiving masters degrees

NAME
Karim Afazul
Mehdi Ahmadi
Total Number: **2**

Names of personnel receiving PHDs

NAME
Huijin He
Total Number: **1**

Names of other research staff

NAME	PERCENT_SUPPORTED
FTE Equivalent:	
Total Number:	

Sub Contractors (DD882)

1 a. Sponsored Programs, University of Nebraska-Lincoln

1 b. 312 N. 14th St, Alexander West

Lincoln NE 68588

Sub Contractor Numbers (c):

Patent Clause Number (d-1):

Patent Date (d-2):

Work Description (e): Extend the present modeling capability to include materials with strong piezoelectric cou

Sub Contract Award Date (f-1): 9/1/10 12:00AM

Sub Contract Est Completion Date(f-2): 8/31/14 12:00AM

Inventions (DD882)

Scientific Progress

1. Measurement of linear and nonlinear material constants of langasite single crystals

We have measured the second-order elastic constants of langasite single crystals and published a conference paper in [1]; a journal paper on this topic is in preparation. We have developed a new experiment setup for determining the third-order elastic constants of single crystals and published this experiment method in [2]. We have obtained all necessary experimental data for the extraction of the third-order elastic constants of a langasite single crystal. The data includes 22 wave speed vs. mechanical loading slopes and zero load wave speeds. However, we found that the calculation result of the 14 third-order elastic constants is not very consistent, for instance, the application of 22 groups of data and 18 groups of data will result in different third-order elastic constants. This is an area that we need to address in the next step. A least-square algorithm that could find the global minimum is required to resolve this issue. Due to this problem, we have developed another new resonator method to determine the third-order elastic constants and third-order piezoelectric, dielectric, and electrostrictive constants. This new method analyzed the contribution of each nonlinear material constants to the nonlinear effect and by optimal design of resonators, the nonlinear material constants could be extracted separately. This method has been published in [3] and [4].

2. Measurement of nonlinear effect of langasite resonators

We have measured the force-frequency and electric field-frequency effects for langasite resonators. The results show some discrepancy between the experimental measurement and theoretical calculations which suggest further investigation on the nonlinear material constants is needed. The results were published in [5] and [6]. The measured force-frequency and electric field-frequency effect have led to two conference proceedings on wireless force sensor [7] and electric field sensor [8] using langasite resonators. In addition to the force-frequency and electric-field frequency measurements, we have measured the drive level dependence (DLD) of langasite resonators with different configurations. The results show that the resonator configuration affects the DLD of the langasite resonator. The DLD measurement results for langasite have been compared with literature values for quartz, langasite, and langatate, and with additional new measurements for a $GaPO_4$ resonator of type R-30 (-11.1° rotated Y-cut). We have also, for the first time, performed an uncertainty analysis for the measured drive level sensitivity. The result has led to a journal paper in [9].

3. Analysis of a surface acoustic wave quartz/langasite resonator

Stress-induced surface acoustic wave velocity shifts are analyzed for langasite (LGS) SAW resonators. The analytical methodology has been verified by comparing experimental results and analytical results for quartz resonators. LGS SAW resonators with Euler angles, which are most sensitive and least sensitive to diametrical forces, are determined and their applications in force sensors and resonators with minimum acceleration sensitivity are discussed. Sensitivity of the analytical results to different groups of nonlinear material constants is discussed; it was found that for specific configurations, failure to include the third-order piezoelectric constants, dielectric constants and electrostrictive constants may lead to a significant calculation error. Surface acoustic waves propagating on an LGS square plate subject to bending moment along the propagation direction and normal to the propagation direction are analyzed; it was found that the average moment-induced velocity shift of LGS resonators are comparable to quartz resonators. Analyses of the sensitivity of the results to different groups of nonlinear material constants show that for some specific wave propagation directions, failure to include the third-order piezoelectric constants, dielectric constants, and electrostrictive constants may lead to large errors. The result has led to a journal publication in [10].

4. Analysis of multi-layer Aluminum Nitride thin film resonators

We have performed a theoretical analysis for a two-layered and mulitlayer zig-zag c-axis inclined zinc oxide thin film resonator. We derived the frequency equation and mode shape for these resonators based on the linear piezoelectric theory. The impedance characteristics of the Thin Film Bulk Acoustic Wave Resonator (FBAR) are derived and compared with previous experimental results. The result has led to two journal papers in [11] and [12]. The application of our analysis led to another journal paper on automotive oil viscosity sensor [13].

5. Analysis of wide-band piezoelectric energy harvesters

Traditional piezoelectric energy harvesters operate in a single resonant frequency. If the excitation frequency is out of the operation frequency range, the energy harvester will fail to generate meaningful energy. We have developed a new multi-beam piezoelectric energy harvester to overcome this barrier. The energy harvester we proposed features 8 times wider operational frequency bandwidth and has an immediate impact on piezoelectric energy harvester design. The result led to two journal publications in [14] and [15].

6. Free vibration of quartz resonators

New results for a better understanding of the design of a thickness-shear mode AT-cut quartz crystal resonator were obtained by studying a series of free vibration problems.

The specific problems analyzed are summarized below.

A rectangular trapped energy resonator partially electroded at the center with rectangular electrodes was analyzed in [16]. A single-mode, three-dimensional equation governing the thickness-shear displacement was used. A Fourier series solution was obtained. The effects of the electrode size and thickness on the trapped modes were examined. Results show the vibration of the trapped thickness-shear modes is mainly under the electrodes and decays rapidly outside the electrodes.

Shear-horizontal free vibrations of an elastic cylinder with an oblate elliptical cross section and a traction-free surface were studied in [17]. It can represent a contoured resonator. The exact vibration modes and frequencies were obtained. The energy-trapping behavior of these modes was examined, and the results show trapped thickness-shear and thickness-twist modes.

Straight-crested waves and vibration modes with variations along the x3 direction only in an AT-cut quartz plate resonator near the operating frequency of the fundamental thickness-shear mode were analyzed in [18]. Previous researchers mainly analyzed x1-dependent modes. Mindlin's two-dimensional equations for anisotropic crystal plates were used. Dispersion relations and frequency spectra of the five relevant waves were obtained. Certain known values of the plate length/thickness ratio needed to be excluded to avoid unwanted couplings between the resonator operating mode and other undesirable modes. Research showed that an additional series of discrete values of the plate length/thickness ratio also needed to be excluded. For overtone modes, the exact frequency spectra for x3-dependent modes were obtained in [19].

A series of new theoretical results on thickness-shear and thickness-twist frequencies and modes were obtained using the scalar differential equations by Tiersten-Smythe and Stevens-Tiersten. These results include the solutions of a circular resonator [20], a rectangular trapped energy resonator [21], and two different contoured resonators [22], [23].

7. Electrically forced vibration

A theoretical analysis on electrically forced vibration of the thickness-shear vibration of a resonator with couplings to both flexure and face-shear modes was performed in [24]. Mindlin's two-dimensional equations for piezoelectric plates were employed. Electrically forced vibration solutions were obtained for three cases: pure thickness-shear mode alone; two coupled modes of thickness shear and flexure; and three coupled modes of thickness shear, flexure, and face shear. The admittance was calculated and its dependence on the driving frequency and the length/thickness ratio of the resonator was examined. Results show that near the thickness-shear resonance, the admittance assumes maxima, and that for certain values of the length/thickness ratio, the coupling to flexure causes severe admittance drops, while the coupling to the face-shear mode causes additional admittance changes previously unknown and unconsidered in current resonator design.

8. Transient effects

Most of the theoretical results on quartz resonators in the literature are for time-harmonic vibrations. We analyzed electrically forced, transient thickness-shear vibration of a quartz resonator [25]. A trigonometric series solution was obtained with which a few transient effects in a piezoelectric resonator under a sudden change or fluctuation of the driving voltage amplitude or frequency were calculated and examined. It was found that, for a 1.65 MHz resonator with a material Q=105, under a sudden change of the driving voltage amplitude, the transition of the resonator vibration takes about 0.1 s, and that a 10 Hz deviation of the driving frequency from the fundamental resonance causes a significant drop of the vibration amplitude. The analysis in [25] was complicated. A much simpler method, which was developed later in [26], can describe the amplitude evolution of transient thickness-shear vibrations of a quartz resonator efficiently and accurately.

9. Second-order in-plane acceleration sensitivity

We also performed a theoretical analysis on the second-order in-plane acceleration sensitivity of a Y-cut quartz thickness-shear mode resonator. The second-order nonlinear theory of elasticity for anisotropic crystals was used to determine the biasing fields in the resonator under in-plane acceleration. The acceleration-induced frequency shift was determined from a perturbation analysis based on the plate equations for small-amplitude vibrations superposed on a finite bias. For a structurally symmetric resonator under in-plane acceleration, although its first-order acceleration-induced frequency shift is known to be zero, its second-order frequency shift was found to be nonzero and is quadratic in the acceleration. An estimate of the second-order frequency shift is found to be of the order of =10-18, 10-16, and 10-14 when the acceleration is 1 g, 10 g, and 100 g, respectively. The result will be submitted to a journal for publication.

10. The developed software package

The "Crystal resonator design and analysis system" software package is based on MATLAB programming language. The software requires MATLAB 2011 or above to run. This software package helped shorten the design cycle of a military electronic system by improving the resonator design efficiency. The software has three major modulus-Material transform modulus, "frequency and mode shape analysis modulus" and "frequency stability analysis modulus".

11. Assessment of langasite for electronic system components

We have measured extensively some nonlinear linear effect for langasite crystal resonators mentioned in Section 2 of this report. These nonlinear effect includes force frequency effects, electroelastic effect and drive level dependence. Here we provide an assessment of this material for electronic system component based on our measurement results:

a. For the force-frequency effect measurements, we have concluded that the langasite resonators have a relatively lower force-frequency effect compared with quartz resonators, which makes them a better candidate for stress compensated resonators which has lower phase noise. This type of resonators is ideal for vehicle-borne or airborne electronic device such as GMTI (Ground Moving Target Indicator). The Minimum Detectable Velocity (MDV) of GMTI is limited by phase noise of the crystal oscillators mounted on it. With the langasite resonator, the MDV-one of the major performance benchmark of a GMTI, could be improved significantly. In addition, langasite resonators could extend the limit of airborn communication systems. Since the noise from a transmitter in one channel extends to neighboring channels, as the number of transmitter grows, the noise can accumulate to the point at which receivers can no longer function properly. For instance, the noise from a typical commercial quartz oscillator (with 2× /g vibration sensitivity) limits the number of users to less than 100 per transponder. Low-phase noise langasite resonators can allow as many as 1200 users per transponder. However, although we have seen the promising application of langasite resonators to military and civil electronic systems, we have not been able to measure the acceleration sensitivity and characterize the phase noise yet, and we have not measured the influence of vibration to the resonant frequency. If further funding is available, we will measure the acceleration sensitivity and phase noise of langasite resonators, which will make us move significantly toward the real application in electronic systems. Langasite also has a very good high temperature performance as its piezoelectricity will remain till its melting point around 1400 deg C, which make it very promising for high temperature sensing application such as pressure and temperature sensing in harsh environments. The application aspects are broad such as the monitoring of jet engines and aerospace propulsion system, or the monitoring of coal/gas-fired power plants, et. Al.

b. For the electroelastic effect (electric field-frequency) measurements, the most important discovery is that we find that the langasite resonators generally have one-order-of -magnitude larger electric field-frequency effect compared with traditional quartz resonators. This new discovery will enable a highly sensitive MEMS resonant electric field sensor that has the benefits of high stability, low cost, low hysteresis, low power and a simple structure. It can be used for the measurement of both DC and AC electric fields with high sensitivity.

c. For the drive level dependence (DLD) measurements, the measured langasite resonators exhibit higher DLD compared with quartz resonators, further experiments and modelling for DLD of langasite resonators with other cut angles are needed to make a more solid conclusion.

Papers published

[1] J. A. Kosinski, H. F. Zhang, Y. Y. Bao, “Measurement of the Second Order Elastic Constant of Langasite Crystals,” ASME 2014 Conference on Smart Materials, Adaptive Structures and Intelligent Systems, Newport, RI, 2014, accepted.
[2] H. F. Zhang, J. A. Kosinski, and K. Afazul, “Apparatus for measurement of acoustic wave propagation under uniaxial loading with application to measurement of third-order elastic constants of piezoelectric single crystals,” Review of Scientific Instrument, vol. 84, pp. 054901-1-5, 2013.
[3] H. F. Zhang, “Optimal cuts to extract the third-order elastic constants of langasite single crystals,” IEEE Transaction on Ultrasonics, Ferroelectrics and Frequency Control, vol. 58, pp. 1245-1254, 2011.
[4] H. F. Zhang, “Optimal Cuts to extract the third-order piezoelectric constants and electrostictive constants of langasite single crystals through the electroelastic effect,” IEEE Transaction on Ultrasonics, Ferroelectrics and Frequency Control, vol. 60, pp. 1453-1466, 2013.
[5] H. F. Zhang, J. A. Turner, J. S. Yang and J. A. Kosinski, “Experimental measurements of the force-frequency effect of thickness mode langasite resonators,” IEEE Transaction on Ultrasonics, Ferroelectrics and Frequency Control, vol. 60, pp. 1475-1478, 2013.
[6] H. F. Zhang, J. A. Turner, J. S. Yang and J. A. Kosinski, Y. Y. Bao*, “Experimental measurement of the electroelastic effect in thickness mode langasite resonators,” IEEE Transaction on Ultrasonics, Ferroelectrics and Frequency Control, vol. 60, pp. 970-974, 2013.
[7] H. F. Zhang, Tinghui Fan*, “Wireless electric field sensor based on a langasite resonator,” Proceedings of IEEE International Frequency Control Symposium, 458 – 461, 2013.
[8] H. F. Zhang, Benjamin D. Montz, Tinghui Fan* and John A. Kosinski, “Wireless langasite resonator as a force sensor,” Proceedings of IEEE International Frequency Control Symposium, 1-6, 2012.
[9] H. F. Zhang, J. A. Kosinski, Y. Xie*, and J. A. Turner, “Drive level dependence of doubly rotated langasite resonators with different configurations,” IEEE Transaction on Ultrasonics, Ferroelectrics and Frequency Control, vol. 60, pp.963-969, 2013.

[10] H. F Zhang, J. A. Kosinski, “Analysis of contributions of nonlinear material constants to stress-induced velocity shifts of quartz and langasite surface acoustic wave resonators, IEEE Transaction on Ultrasonics, Ferroelectrics and Frequency Control, vol. 60, pp. 975-985, 2013.
[11] H. F. Zhang, J. A. Kosinski, “Analysis of thickness vibrations of C-Axis inclined zig-zag two-layered zinc oxide thin film resonators,” IEEE Transaction on Ultrasonics, Ferroelectrics and Frequency Control, vol. 59, pp. 2831-2836, 2012.
[12] H. F. Zhang, “Analysis of thickness vibrations of C-Axis inclined Zig-Zag multi-layered zinc oxide thin film resonators,” Ferroelectrics, vol. 445, pp. 96-106, 2013.
[13] H. F. Zhang and Y. Y. Bao*, “Sensitivity analysis of multi-layered C-Axis inclined Zig-zag zinc oxide thin film resonators as a viscosity sensor,” IEEE Transaction on Ultrasonics, Ferroelectrics and Frequency Control, vol. 61, pp. 525-534, 2014.
[14] H. F. Zhang and K. Afazul, “Design and analysis of a connected broadband multipiezoelectric bimorph beams energy harvester,” IEEE Transaction on Ultrasonics, Ferroelectrics and Frequency Control, vol. 61, pp. 1016-1023, 2014.
[15] H. F. Zhang and M. Ahmadi, “Resonance tuning of a multi-piezoelectric bimorph beams energy harvester connected by springs,” Ferroelectrics, vol. 460, pp. 34-48, 2014.
[16] H. J. He, J. S. Yang, J. A. Kosinski and J. Wang, Thickness-shear vibration of a rectangular quartz plate with partial electrodes, Acta Mechanica Solida Sinica, vol. 26, pp. 121-128, 2013.
[17] H. J. He, J. S. Yang and J. A. Kosinski, Shear-horizontal vibration modes of an oblate elliptical cylinder and energy trapping in contoured acoustic wave resonators, IEEE Trans. Ultrason., Ferroelect., Freq. Contr., vol. 59, pp. 1774-1780, 2012.
[18] G. J. Chen, R. X. Wu, J. Wang, J. K. Du and J. S. Yang, Five-mode frequency spectra of x3-dependent modes in AT-cut quartz resonators, IEEE Trans. Ultrason., Ferroelect., Freq. Contr., vol. 59, pp. 811-816, 2012.
[19] J. Zhu, W. Q. Chen and J. S. Yang, Overtone frequency spectra for x3-dependent modes in AT-cut quartz resonators, IEEE Trans. Ultrason., Ferroelect., Freq. Contr., vol. 60, pp. 858-863, 2013.
[20] H. J. He, J. S. Yang and Q. Jiang, Thickness-shear and thickness-twist vibrations of circular AT-cut quartz resonators, Acta Mechanica Solida Sinica, vol. 26, pp. 245-254, 2013.
[21] J. J. Shi, C. Y. Fan, M. H. Zhao and J. S. Yang, Variational formulation of the Stevens-Tiersten equation and application in the analysis of rectangular trapped-energy quartz resonators, J. Acoust. Soc. Am., vol. 135, pp. 175-181, 2014.
[22] P. Li, F. Jin and J. S. Yang, Thickness-shear vibration of an AT-cut quartz resonator with a hyperbolic contour, IEEE Trans. Ultrason., Ferroelect., Freq. Contr., vol. 59, pp. 1006-1012, 2012.
[23] W. J. Wang, R. X. Wu, J. Wang, J. K. Du and J. S. Yang, Thickness-shear modes of an elliptic, contoured AT-cut quartz resonator, IEEE Trans. Ultrason., Ferroelect., Freq. Contr., vol. 60, pp. 1192-1198, 2013.
[24] H. J. He, J. S. Yang, W. P. Zhang and J. Wang, Effects of mode coupling on the admittance of an AT-cut quartz thickness-shear resonator, Chinese Physics B, vol. 22, pp. 047702, 2013.
[25] N. Liu, J. S. Yang and F. Jin, Transient thickness-shear vibration of a piezoelectric plate of monoclinic crystals, Int. J. of Applied Electromagnetics and Mechanics, vol. 38, pp. 27-37, 2012.
[26] Z. Wang, M. H. Zhao and J. S. Yang, Amplitude evolution equation and transient effects in piezoelectric crystal resonators, J. Appl. Phys., pp. 114, pp. 144510, 2013.

Technology Transfer

Introduction of the Crystal resonator design and analysis system software

The “Crystal resonator design and analysis system” is software based on MATLAB programming language. The software requires MATLAB 2011 or above to run. This software package helped shorten the design cycle of a military electronic system by improving the resonator design efficiency. The software has three major modulus-Material transform modulus, “frequency and mode shape analysis modulus” and “frequency stability analysis modulus”. The material transform modulus converts the material constants including second-order and third-order elastic constants, piezoelectric constants, dielectric constants, and electrostrictive constants to a new coordinate system. By simply inputting the rotation angle Φ, Θ, Ψ, user would be able to calculate the new second-order and third-order elastic constants for both quartz and langasite single crystals, the detailed introduction is in a separate file-Instruction-Material constant transformation.docx.

The frequency and mode shape analysis modulus calculate the resonant frequency and plot the mode shape for both bulk acoustic wave (BAW) and surface acoustic wave (SAW) resonators. It included three sub-modulus-“SC cut analysis modulus”, “AT cut analysis modulus” and “Rayleigh wave analyses modulus”. The SC cut analysis modulus allow users to define the resonator geometry for either rectangular or circular shape, it also provided electrode or unelectroded options. After defining resonator geometry and mode order, the user could plot the 3-D resonator mode shape and resonant frequency. The detailed introduction can be found in a separate file-Instruction-Contourresonator.docx.

Similar to the SC cut analysis modulus, the AT cut analysis modulus allow users to define resonator shape, geometry, electrode condition and plot resonator mode shape and determine the resonant frequency, the detailed introduction can be found in a separate file-Instruction-Contourresonator.docx.

The Rayleigh wave analysis modulus performs the saw wave frequency or wave length calculations and plot the related wave mode. It allows user to select wave frequency calculation or wave length calculations. The detailed theoretical background can be found in a separate file-Instruction-Rayleighwave.docx

The frequency stability analysis modulus includes three sub-modulus-acceleration sensitivity modulus, temperature effect modulus and electric field frequency modulus. The acceleration sensitivity modulus allows users to define the resonator geometry, mode order, and material orientation and calculate the acceleration sensitivity, the detailed theoretical background can be found in a separate file- Instruction-accelerationsensitivity.docx.

The temperature frequency and electric field frequency modulus will be developed in future.

Software installation

Firstly, set up a new folder in C drive, the name of the folder should be CRDV1 .

C:\CRDV1

Secondly, please copy all files into the folder (C:\CRDV1)

Thirdly, click the Controlplatform.fig to run the whole program.

Material constant transformation

The foundation for the material constants transformation is based on tensor transformation principle.

$$t'_{kmp..} = Q_{lk}Q_{nm}Q_{qp} \dots t_{lnq\dots}$$

While Q is the material rotation matrix. The second-order elastic, piezoelectric and dielectric constants were transformed to new coordinate (Fig.1) and are shown in the front panel. The third-order elastic, piezoelectric, dielectric constants and electrostricitive constants are transformed to the new coordinate as well. Due the large number of these nonlinear constants, the transformed constants are stored in a file "mydata.mat" when click the "save" button in the front panel. Users can access all transformed constants by loading this file in the MATLAB command window.

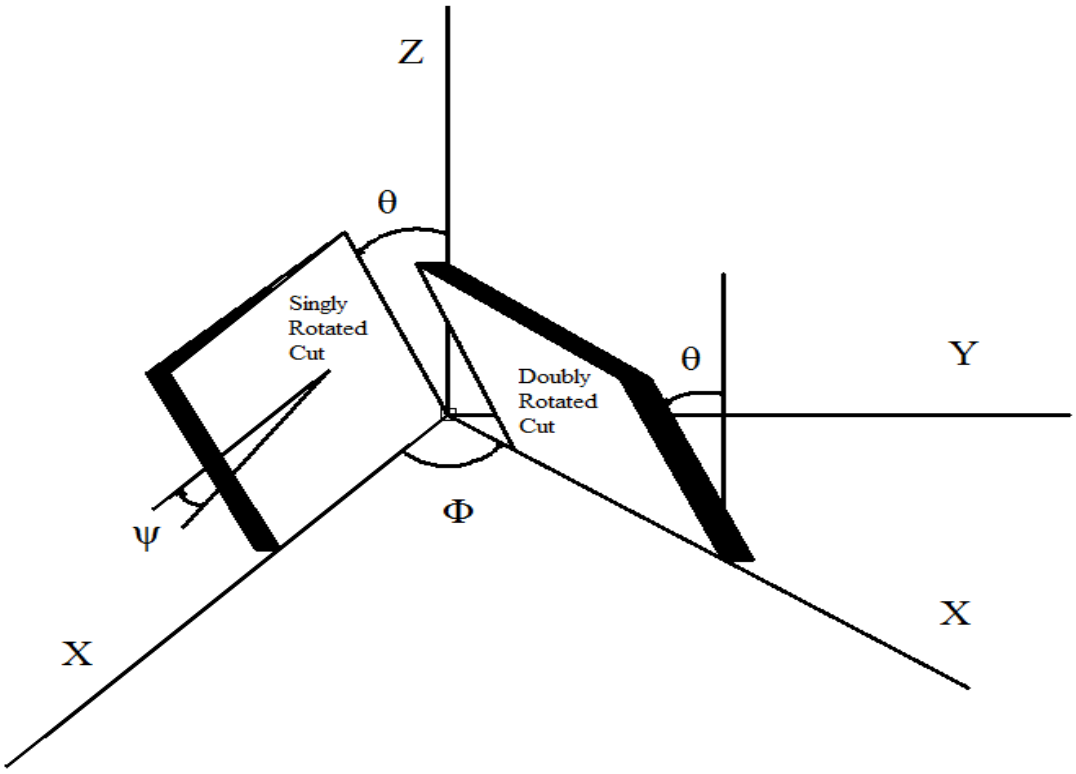

Fig. 1. Plate orientations.

Instructions

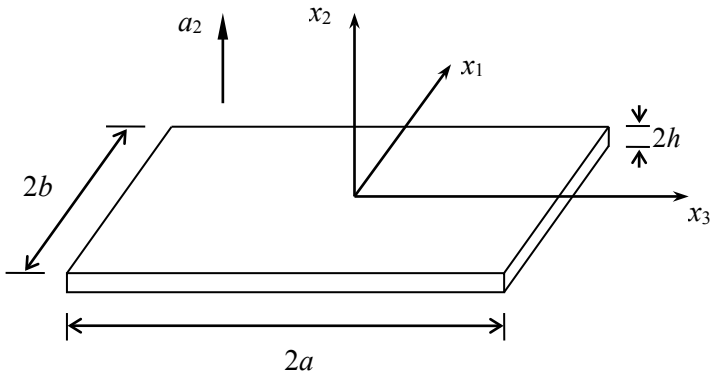

Figure 1. A simply supported rectangular plate under normal acceleration.

Purpose: Calculating the displacement gradient field of the biasing deformation in a simply supported, AT-cut quartz plate under normal acceleration.

Input:
a —half of the plate length (unit: mm),
b — half of the plate width (unit: mm),
h — half of the plate thickness (unit: mm),
a_2 — normal acceleration (unit: m/s^2).
Output:
$w_{i,j}$— displacement gradient (unit: 10^{-6}), i, j =1, 2, 3.

The deflection $w_2^{(0)}(x_1, x_3)$ of a simply supported plate induced by normal acceleration is governed by [1]:

$$\frac{2}{3}h^3\gamma_{ABCD}w_{2,CDAB}^{(0)} + 2\rho h a_2 = 0\,,\ A,\ B,\ C,\ D\ =1,\ 3. \tag{1}$$

The boundary conditions are:

$$w_2^{(0)} = 0\,,\ \ K_{11}^{(1)} = 0\,,\ \text{at}\ \ x_1 = \pm a\,, \tag{2}$$

$$w_2^{(0)} = 0\,,\ \ K_{33}^{(1)} = 0\,,\ \text{at}\ \ x_3 = \pm b\,. \tag{3}$$

The solution can be expressed by Fourier series [1]:

$$w_2^{(0)} = \sum_{m=1,3,5}^{\infty}\sum_{n=1,3,5}^{\infty} A_{mn}\cos(\alpha_m x_1)\cos(\kappa_n x_3)\,, \tag{4}$$

where

$$\alpha_m = \frac{m\pi}{2a}\,,\ \ \kappa_n = \frac{n\pi}{2b}\,,\ \ m,\ \ n=1,3,5,\ldots, \tag{5}$$

$$A_{mn} = (-1)^{m+n+1}\frac{48\rho a_2}{mn\pi^2 h^2[\gamma_{11}\alpha_m^4 + \gamma_{33}\kappa_n^4 + (2\gamma_{13}+4\gamma_{55})\alpha_m^2\kappa_n^4]}\,. \tag{6}$$

We note that the A_{mn} in [1] has an error and (6) is believed to be correct. Once $w_2^{(0)}$ is known, we have [1]

$$w_A^{(1)} = -w_{2,A}^{(0)}. \tag{7}$$

Thus the plate strains $E_{CD}^{(1)}$ are given by [1]:

$$E_{CD}^{(1)} = -w_{2,CD}^{(0)}. \tag{8}$$

Other plate strains $E_W^{(1)}$ are given by [1]:

$$E_W^{(1)} = -c_{WV}^{-1} c_{VS} E_S^{(1)},\ R, S = 1, 3, 5,\ W, V = 2, 4, 6, \tag{9}$$

where R, S, W, V are indices in compact index notation. The three-dimensional strain field can be obtained based on (8) and (9) [1]:

$$E_{KL} = x_2 E_{KL}^{(1)}, \tag{10}$$

where K, L=1, 2, 3. The anti-symmetric part of the displacement gradient is:

$$\Omega_{KL} = \frac{1}{2}(w_{L,K} - w_{K,L}). \tag{11}$$

According to [1], Ω_{KL} can be further simplified as:

$$\Omega_{2A} = -w_{2,A}^{(0)} + x_2 E_{2A}^{(1)},\ \ \Omega_{13} = 0. \tag{12}$$

Finally the displacement gradients are given by:

$$w_{K,L} = E_{KL} + \Omega_{LK}. \tag{13}$$

For convenience, we list the displacement gradient of an AT-cut plate as follows:

$$w_{1,1} = x_2 \sum_{m=1,3,5}^{\infty} \sum_{n=1,3,5}^{\infty} A_{mn} \alpha_{\mathrm{m}}^2 \cos(\alpha_m x_1)\cos(\kappa_n x_3),$$

$$w_{1,2} = 0.1744 x_2 \sum_{m=1,3,5}^{\infty} \sum_{n=1,3,5}^{\infty} A_{mn} \alpha_m \kappa_n \sin(\alpha_m x_1)\sin(\kappa_n x_3) + \sum_{m=1,3,5}^{\infty} \sum_{n=1,3,5}^{\infty} A_{mn} \alpha_m \sin(\alpha_m x_1)\cos(\kappa_n x_3),$$

$$w_{1,3} = -x_2 \sum_{m=1,3,5}^{\infty} \sum_{n=1,3,5}^{\infty} A_{mn} \alpha_m \kappa_n \sin(\alpha_m x_1)\sin(\kappa_n x_3),$$

$$w_{2,1} = \sum_{m=1,3,5}^{\infty} \sum_{n=1,3,5}^{\infty} A_{mn} \alpha_m \sin(\alpha_m x_1)\cos(\kappa_n x_3),$$

$$w_{2,2} = 0.0598 x_2 \sum_{m=1,3,5}^{\infty} \sum_{n=1,3,5}^{\infty} A_{mn} \alpha_m^2 \cos(\alpha_m x_1)\cos(\kappa_n x_3) + 0.0689 x_2 \sum_{m=1,3,5}^{\infty} \sum_{n=1,3,5}^{\infty} A_{mn} \kappa_n^2 \cos(\alpha_m x_1)\cos(\kappa_n x_3),$$

$$w_{2,3} = -\sum_{m=1,3,5}^{\infty} \sum_{n=1,3,5}^{\infty} A_{mn} \kappa_n \cos(\alpha_m x_1)\sin(\kappa_n x_3),$$

$$w_{3,1} = -x_2 \sum_{m=1,3,5}^{\infty} \sum_{n=1,3,5}^{\infty} A_{mn}\alpha_m\kappa_n \sin(\alpha_m x_1)\sin(\kappa_n x_3),$$

$$w_{3,2} = 0.0860x_2 \sum_{m=1,3,5}^{\infty} \sum_{n=1,3,5}^{\infty} A_{mn}\alpha_m^2 \cos(\alpha_m x_1)\cos(\kappa_n x_3) - 0.2671x_2 \sum_{m=1,3,5}^{\infty} \sum_{n=1,3,5}^{\infty} A_{mn}\kappa_n^2 \cos(\alpha_m x_1)\cos(\kappa_n x_3)$$
$$+ \sum_{m=1,3,5}^{\infty} \sum_{n=1,3,5}^{\infty} A_{mn}\kappa_n \cos(\alpha_m x_1)\sin(\kappa_n x_3),$$

$$w_{3,3} = x_2 \sum_{m=1,3,5}^{\infty} \sum_{n=1,3,5}^{\infty} A_{mn}\kappa_n^2 \cos(\alpha_m x_1)\cos(\kappa_n x_3).$$

Once the displacement gradients are determined, they will be substituted into the perturbation integral (14) to calculate the frequency shift caused by acceleration [2]. In our program, only second and third-order elastic constants are included in the calculation, all other nonlinear constants such as third-order dielectric, piezoelectric, electrostrictive constants are ignored.

$$\Delta\omega_M = \omega - \omega_M = \frac{1}{2\omega_M \int \rho_0 (u_1^M u_1^M + u_2^M u_2^M + u_3^M u_3^M) dV} \times \int_V (\hat{c}_{K\alpha L\gamma} u^M_{\gamma,K} u^M_{\alpha,L} + 2\hat{e}_{KL\gamma}\phi^M_K u^M_{\gamma,L} - \hat{\varepsilon}_{KL}\phi^M_{,K}\phi^M_{,L}) dV, \quad (14)$$

where

$$\begin{aligned}
\hat{c}_{K\alpha L\gamma} &= T^0_{KL}\delta_{\alpha\gamma} + c_{K\alpha LN} w_{\gamma,N} + c_{KNL\gamma} w_{\alpha,N} \\
&\quad + c_{K\alpha L\gamma AB} S^0_{AB} + k_{AK\alpha L\gamma} E^0_A, \\
\hat{e}_{KL\gamma} &= e_{KLM} w^0_{\gamma,M} - k_{KL\gamma AB} S^0_{AB} + b'_{AKL\gamma} E^0_A, \\
\hat{\varepsilon}_{KL} &= b'_{KLAB} S^0_{AB} + \chi_{KLA} E^0_A,
\end{aligned}$$

with

$$b'_{AKL\gamma} = b_{ABCD} + \varepsilon_0\delta_{AB}\delta_{CD} - \varepsilon_0(\delta_{AC}\delta_{BD} + \delta_{AD}\delta_{BC}).$$

Where, ω_M is the unperturbed angular frequency, ω is the perturbed angular frequency, and $\Delta\omega_M$ is the angular frequency shift. Here, $\hat{c}_{K\alpha L\gamma}$, $\hat{e}_{KL\gamma}$, and $\hat{\varepsilon}_{KL}$ are the effective elastic, piezoelectric, and dielectric constants respectively; u^M_γ is a specific mode shape function in the unperturbed condition and ϕ^M is the electrical potential for this specific mode.

, , are the initial stress, strain and electrical field respectively with $w_{\gamma,N}$ defining the displacement gradient. $c_{K\alpha L\gamma}$, d_{fAB}, ε_{KL} are the second-order elastic, piezoelectric and dielectric constants. $c_{K\alpha L\gamma AB}$, $k_{fK\alpha L\gamma}$, and χ_{KLf} are the third-order elastic, piezoelectric, and dielectric constants respectively and $b_{fAL\gamma}$ are the electrostrictive constants. ε_0 is the

permittivity of free space.

References

1. H. F. Tiersten and D. V. Shick, “On the normal acceleration sensitivity of ST-cut quartz surface wave resonators supported along rectangular edges,” Journal of Applied Physics, vol. 64, no. 9, pp. 4334-4341, 1988.
2. H. F. Tiersten, “Perturbation theory for linear electroelastic equations for small Fields superposed on a bias,” J. Acoust. Soc. Am, vol. 64, pp. 832—837, 1978.

Instruction

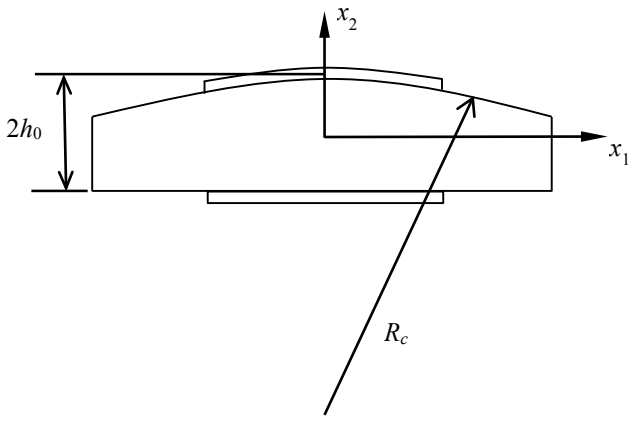

Figure 1. A Contoured resonator and coordinate system.

Purpose:
Calculating free vibration frequencies and modes of AT- or SC-cut bi-convex or plano-convex quartz resonators, either unelectroded or fully electroded.

Input:
$2h_0$ — resonator center thickness.
R — electrode/resonator mass ratio=$\rho' 2h'/(\rho h_0)$. ρ'=electrode mass density. $2h'$: electrode thickness.
R_c — radius of curvature of the convex surface of a plano-convex resonator, or half of the radius of curvature of the convex surface of a bi-convex resonator.
n=1, 3, 5, … — number of nodal points of the mode along the resonator thickness direction x_2.
m=0, 2, 4 — mode order along the in-plane direction x_1 determined by the Hermite polynomial solutions $H_m(x_1)$ of the modes.
p=0, 2, 4 — mode order along the in-plane direction x_3 determined the Hermite polynomial solutions $H_p(x_3)$ of the modes.
D — diameter of a circular resonator.
$2L$ and $2W$ — length along x_1 and width along x_3 of a rectangular resonator.

Output:
Frequency (Hz).
Mode shape: figure.
Mode shape: data array (500 data points along D, or $2L$, or $2W$).

Note:
The frequencies and modes of AT-cut resonators are calculated using Eqs. (3.10) and (3.13) of [1]. The frequencies and modes of SC-cut resonators are calculated using Eqs. (124) and (126) of [2]. The modes and frequencies in [1] and [2] are for resonators unbounded in the x_1-x_3 plane. Since the modes die out quickly away from the center, the output of the modes is calculated within a finite circular or rectangular region predetermined by the user of this computer code.

References:
[1] H. F. Tiersten and R. C. Smythe, “An analysis of contoured crystal resonators operating in overtones of coupled thickness shear and thickness twist,” vol. 65, no. 6, pp. 1455-1460, 1979.
[2] D. S. Stevens and H. F. Tiersten, “An analysis of doubly rotated quartz resonators utilizing essentially thickness modes with transverse variation,” *Journal of the Acoustical Society of America*, vol. 79, no. 6, pp. 1811-1826, 1986.

Instructions

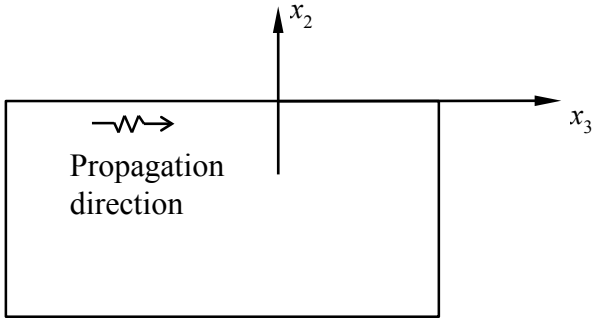

Figure 1. A half space of AT-cut quartz and coordinate system.

Purpose: Calculating the displacement components (u_2 and u_3) of Rayleigh waves propagating along x_3.

Input:
f — wave frequency (MHz) or λ — wavelength (mm).

Output:
λ — wavelength (mm) or f — wave frequency (MHz).
Mode variation along x_2 (figures).
Mode variation along x_2 (data array, 501 data points along x_2).

Theoretical Background:
For Rayleigh waves propagating along the x_3 axis, the governing equations are:

$$\begin{aligned} c_{22}u_{2,22} + 2c_{24}u_{2,23} + c_{44}u_{2,33} + c_{24}u_{3,22} + (c_{23}+c_{44})u_{3,23} + c_{34}u_{3,33} &= \rho\ddot{u}_2 \\ c_{24}u_{2,22} + (c_{23}+c_{44})u_{2,23} + c_{34}u_{2,33} + c_{44}u_{3,22} + 2c_{34}u_{3,23} + c_{33}u_{3,33} &= \rho\ddot{u}_3 \end{aligned} \tag{1}$$

Consider the following solution:

$$\begin{aligned} u_2 &= A\exp(k_2 x_2)\exp i(k_3 x_3 - \omega t) \\ u_3 &= B\exp(k_2 x_2)\exp i(k_3 x_3 - \omega t) \end{aligned} \tag{2}$$

Substituting from (2) into (1) and eliminating the common exponential factor, we obtain:

$$\begin{aligned} (c_{22}k_2^2 + 2c_{24}ik_2k_3 - c_{44}k_3^2 + \rho\omega^2)A + [c_{24}k_2^2 + (c_{23}+c_{44})ik_2k_3 - c_{34}k_3^2]B &= 0 \\ [c_{24}k_2^2 + (c_{23}+c_{44})ik_2k_3 - c_{34}k_3^2]A + (c_{44}k_2^2 + 2c_{34}ik_2k_3 - c_{44}k_3^2 + \rho\omega^2)B &= 0 \end{aligned} \tag{3}$$

For nontrivial solutions, the determinant of the coefficient matrix must vanish, thus

$$\begin{vmatrix} (c_{22}k_2^2 + 2c_{24}ik_2k_3 - c_{44}k_3^2 + \rho\omega^2) & [c_{24}k_2^2 + (c_{23}+c_{44})ik_2k_3 - c_{34}k_3^2] \\ [c_{24}k_2^2 + (c_{23}+c_{44})ik_2k_3 - c_{34}k_3^2] & (c_{44}k_2^2 + 2c_{34}ik_2k_3 - c_{44}k_3^2 + \rho\omega^2) \end{vmatrix} = 0 \tag{4}$$

(4) is a quartic equation for k_2. There are four complex roots. For surface waves the displacements must decay as x_2 approaches minus infinity. Only the two roots with positive real parts denoted by $k_2^{(1)}$ and $k_2^{(2)}$ are taken. The amplitude ratios $\alpha^{(i)}$ are defined by:

$$B^{(i)} = \alpha^{(i)} A^{(i)} \tag{5}$$

where

$$\alpha^{(i)} = -\frac{c_{22}(k_2^{(i)})^2 + 2c_{24}ik_2^{(i)}k_3 - c_{44}k_3^2 + \rho\omega^2}{c_{24}(k_2^{(i)})^2 + (c_{23}+c_{44})ik_2^{(i)}k_3 - c_{34}k_3^2}, \quad i=1, 2 \tag{6}$$

The displacement field can be expressed as:

$$\begin{aligned} u_2 &= [A_1 \exp(k_2^{(1)}x_2) + A_2 \exp(k_2^{(2)}x_2)]\exp i(k_3x_3 - \omega t) \\ u_3 &= [\alpha_1 A_1 \exp(k_2^{(1)}x_2) + \alpha_2 A_2 \exp(k_2^{(2)}x_2)]\exp i(k_3x_3 - \omega t) \end{aligned} \tag{7}$$

The stress components needed for the boundary conditions are calculated from:

$$\begin{aligned} T_{22} &= c_{22}u_{2,2} + c_{23}u_{3,3} + c_{24}(u_{2,3} + u_{3,2}) \\ T_{23} &= c_{24}u_{2,2} + c_{34}u_{3,3} + c_{44}(u_{2,3} + u_{3,2}) \end{aligned} \tag{8}$$

The traction-free boundary conditions are:

$$T_{22} = 0,\ T_{23} = 0, \text{ at } x_2 = 0 \tag{9}$$

The substitution from (7) into (9) through (8) gives

$$\begin{aligned} &[(c_{22}+c_{24}\alpha_1)k_2^{(1)} + (c_{24}+c_{23}\alpha_1)ik_3]A_1 + [(c_{22}+c_{24}\alpha_2)k_2^{(2)} + (c_{24}+c_{23}\alpha_2)ik_3]A_2 = 0 \\ &[(c_{24}+c_{44}\alpha_1)k_2^{(1)} + (c_{44}+c_{34}\alpha_1)ik_3]A_1 + [(c_{24}+c_{44}\alpha_2)k_2^{(2)} + (c_{44}+c_{34}\alpha_2)ik_3]A_2 = 0 \end{aligned} \tag{10}$$

Nontrivial solution of (9) exists if

$$\begin{vmatrix} (c_{22}+c_{24}\alpha_1)k_2^{(1)} + (c_{24}+c_{23}\alpha_1)ik_3 & (c_{22}+c_{24}\alpha_2)k_2^{(2)} + (c_{24}+c_{23}\alpha_2)ik_3 \\ (c_{24}+c_{44}\alpha_1)k_2^{(1)} + (c_{44}+c_{34}\alpha_1)ik_3 & (c_{24}+c_{44}\alpha_2)k_2^{(2)} + (c_{44}+c_{34}\alpha_2)ik_3 \end{vmatrix} = 0 \tag{11}$$

(11) is an equation for the wave speed $v = \omega / k_3$. It has only one root. The corresponding ratio between A_1 and A_2 is determined from (10). A_1=1 is used in the output.